**Supplementary Information**

# Combining sonicated cold development and pulsed electrodeposition for high aspect ratio sub-10-nm gap gold dimers for sensing applications in the visible spectrum

Aaron D. Mueller,[a] Landobasa Y. M. Tobing[a] and Dao Hua Zhang*[a]

School of Electrical and Electronic Engineering, Nanyang Technological University, 50 Nanyang Avenue, S639798. E-mail: edhzhang@ntu.edu.sg

## Detailed measurement of lateral dimer dimensions

The data for the dimer side lengths, $s_x$ and $s_y$, and gaps $g$ were obtained by overlaying bars in respective locations on the SEM images, followed by converting the bar length to a distance based on the scalebar length. Figures S1 through S6 show the images and bar overlays used for these measurements. In Figure S1, the data from the dimers in red boxes were excluded due to the joining of the two individual dimers. In all these figures, the brown bars represent $s_x$, the cyan bars represent $s_y$, and the red bars represent $g$.

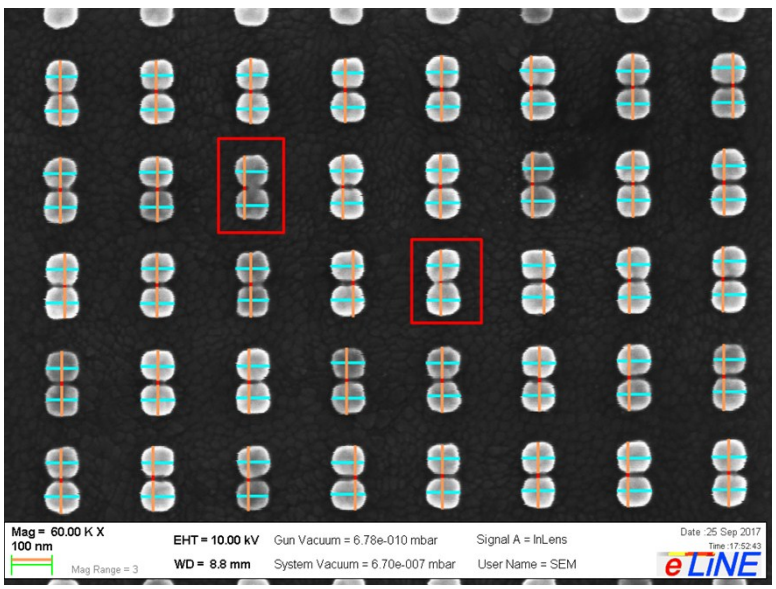


Figure S1. Lateral measurements for the $s_{60}g_{20}$ structures. The dimers in red boxes were excluded from the measurements due to the joining of the individual dimer squares.

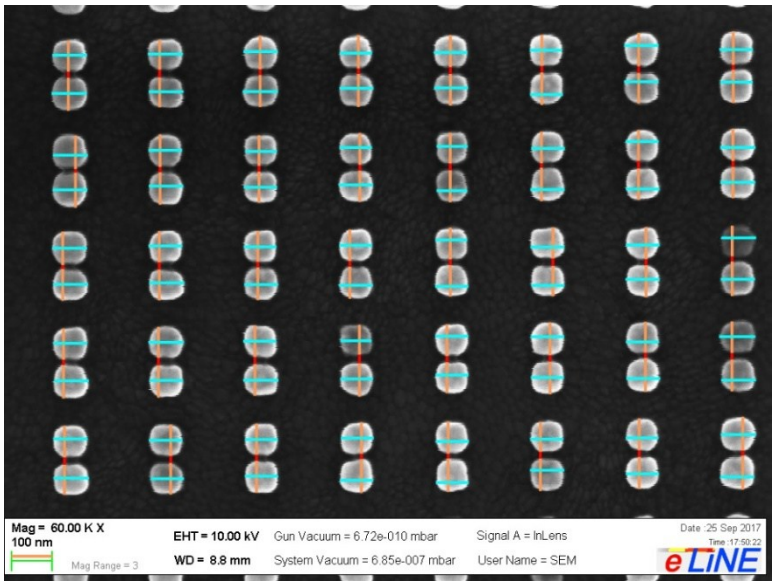


Figure S2. Lateral measurements for the $s_{60}g_{30}$ structures.

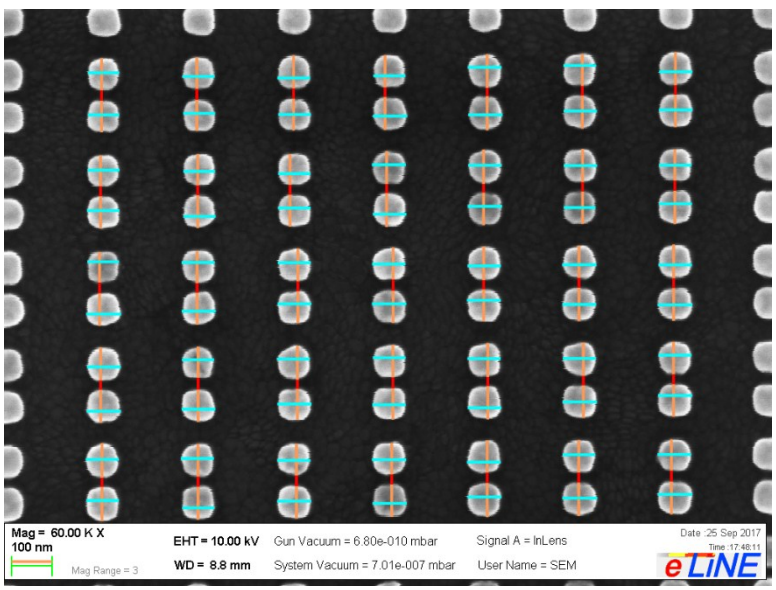


Figure S3. Lateral measurements for the $s_{60}g_{40}$ structures.

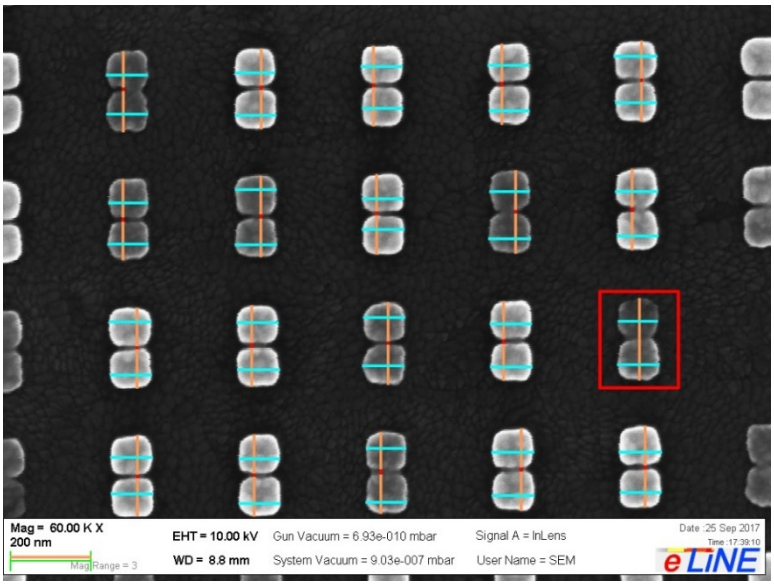


Figure S4. Lateral measurements for the $s_{80}g_{20}$ structures. The dimer in red box was excluded from the measurements due to the joining of the individual dimer squares.

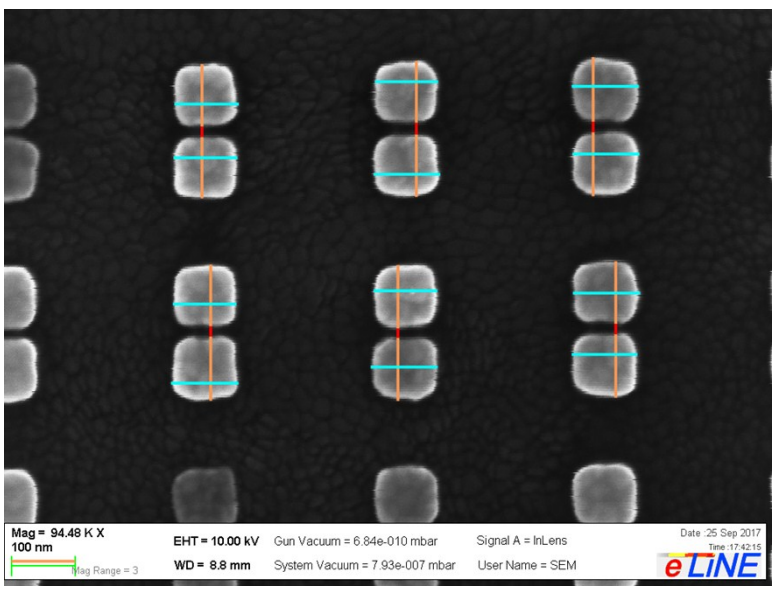


Figure S5. Lateral measurements for the $s_{80}g_{30}$ structures.

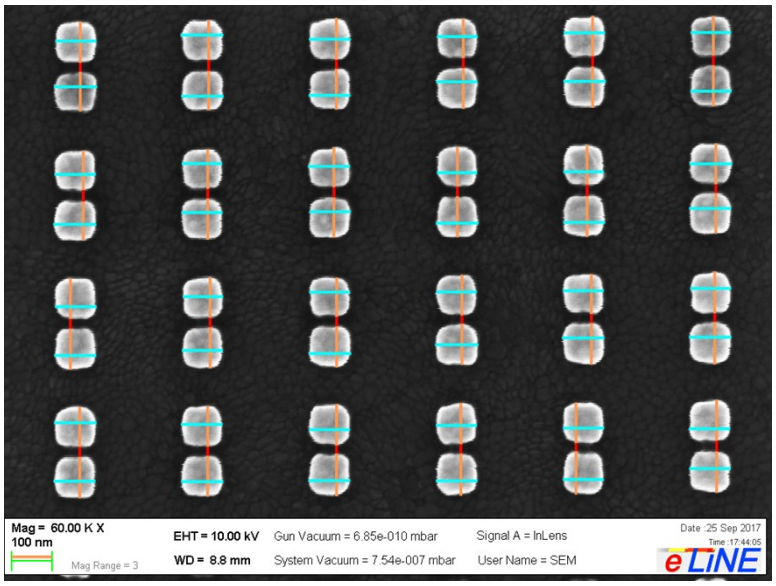


Figure S6. Lateral measurements for the $s_{80}g_{40}$ structures.

## Detailed measurement of dimer heights

For calculation of the heights based on the line segments shown in the oblique-incidence SEM pictures, the following procedure was used. Suppose that before sample rotation, the sample is lying flat in the $xy$ plane. The sample is rotated by an angle of $-\alpha$ about the $z$ axis and then by an angle of $\theta$ (for inclination) about the $x$ axis. Using a product of appropriate rotation matrices, it can be shown that the new directions of the sample axes are given by

$$\hat{x}' = \begin{pmatrix} \cos\alpha \\ -\sin\alpha\cos\theta \\ -\sin\alpha\sin\theta \end{pmatrix},\ \hat{y}' = \begin{pmatrix} \sin\alpha \\ -\cos\alpha\cos\theta \\ -\cos\alpha\sin\theta \end{pmatrix},\ \hat{z}' = \begin{pmatrix} 0 \\ -\sin\theta \\ \cos\theta \end{pmatrix}.$$

Thus, when viewed from the $+\hat{z}$ direction, a structure of height $h_0$ will appear to have a height, based on the $\hat{x}$ and $\hat{y}$ components of $\hat{z}'$, of $|h_{SEM}| = h_0 \sin\theta$. Therefore, we find that the height of the structure is simply given by $h_0 = |h_{SEM}|/\sin\theta$. For our system, the inclination angle was $\theta = 25°$. This corresponds to multiplying the scalebar-normalized heights by a factor of $1/sin\theta \cong 2.366$ . The oblique SEM images with overlaid scalebars are shown below in Figures S7-S12.

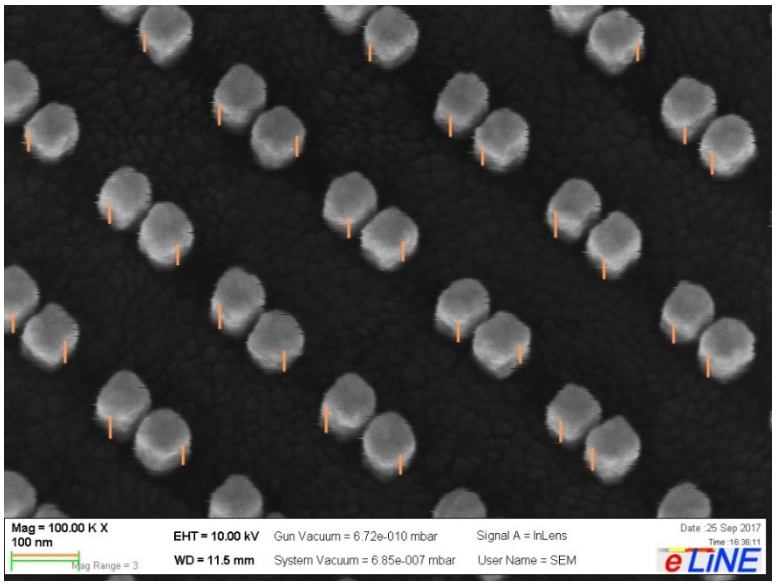


Figure S7. Height measurements for the $s_{60}g_{20}$ structures.

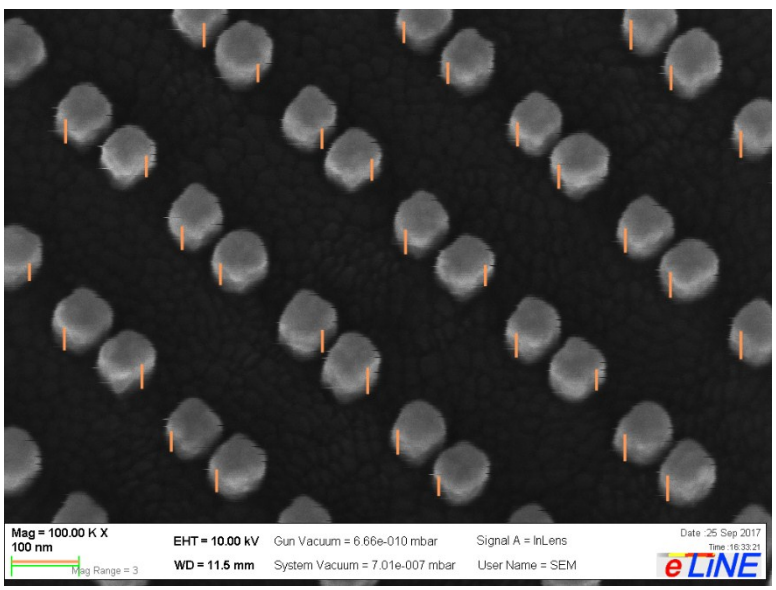


Figure S8. Height measurements for the $s_{60}g_{30}$ structures.

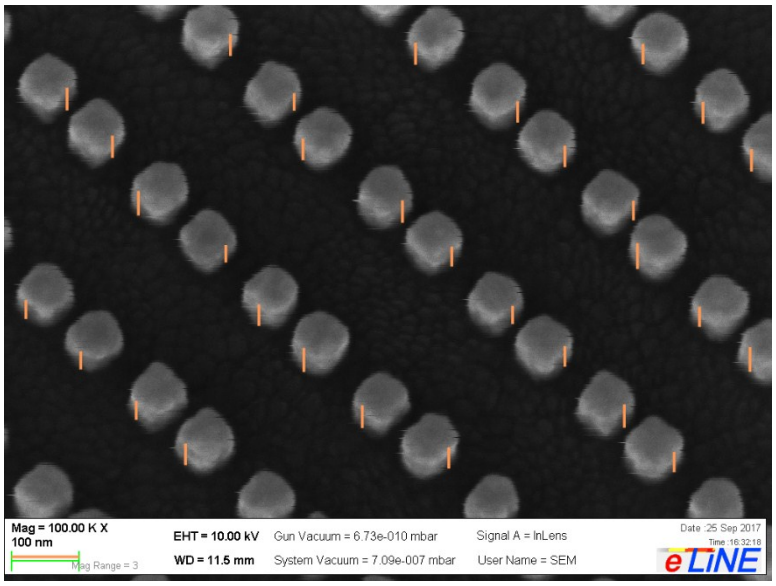


Figure S9. Height measurements for the $s_{60}g_{40}$ structures.

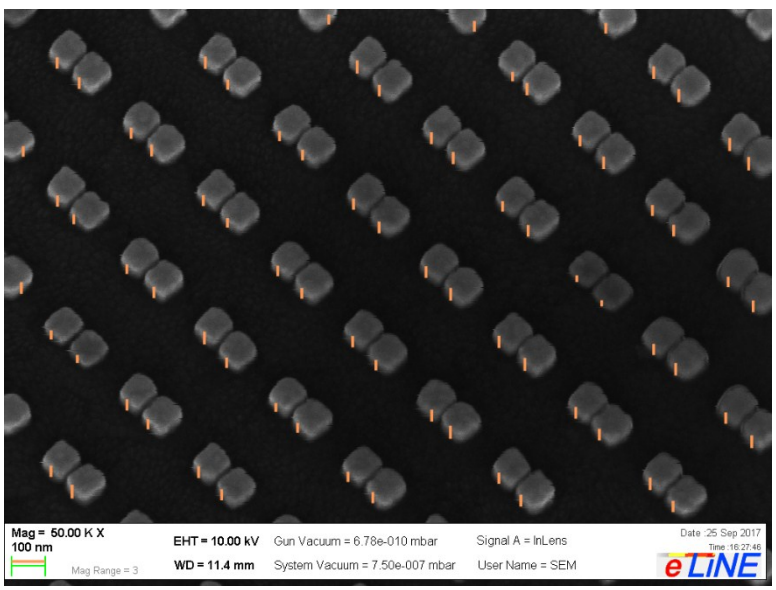


Figure S10. Height measurements for the $s_{80}g_{20}$ structures.

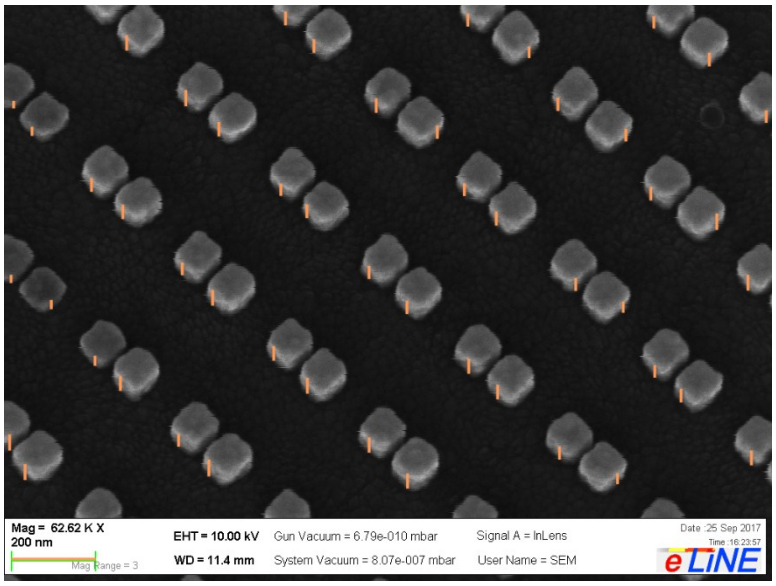


Figure S11. Height measurements for the $s_{80}g_{30}$ structures.

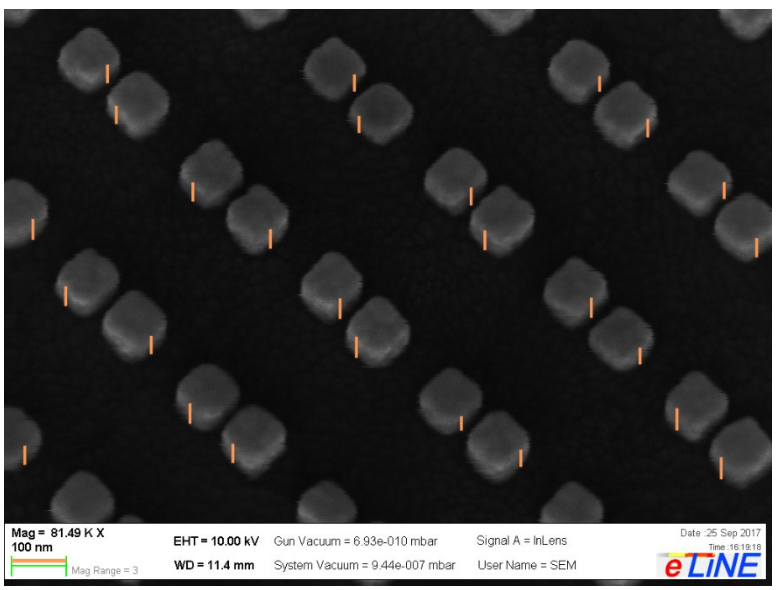


Figure S12. Height measurements for the $s_{80}g_{40}$ structures.

## Blue Shift of Transverse Modes as Structure Height Increases

Localized surface plasmon resonance is strongly dependent on nanostructure geometry. Here we assume a nanostructure of fixed cross-section and variable height $h$, with one end supported by a substrate. When $h$ becomes on the order of $\lambda/2n_{eff}$, the structure may be able to support so-called *longitudinal* modes, which may propagate vertically along the structures, akin to a Fabry-Perot resonance which satisfies the round-trip phase condition $2k_0 n_{eff} h + \phi_{air} + \phi_{ITO} = 2m\pi$. For this work,

the resonance modes of interest are such that $h \ll \lambda/2n_{eff}$. As these modes are not longitudinal, we refer to them as *transverse* modes, similar to modes of traditional planar metallic nanoparticles. Despite their transverse nature, the resonance wavelength $\lambda_{LSPR}$ still exhibits some dependence on structure height, as seen experimentally and verified using FDTD simulations, which are shown below in Figure S13. The resonance wavelength decreases as height increases. The explanation for this blueshift in terms of electromagnetic theory is beyond the scope of this work.

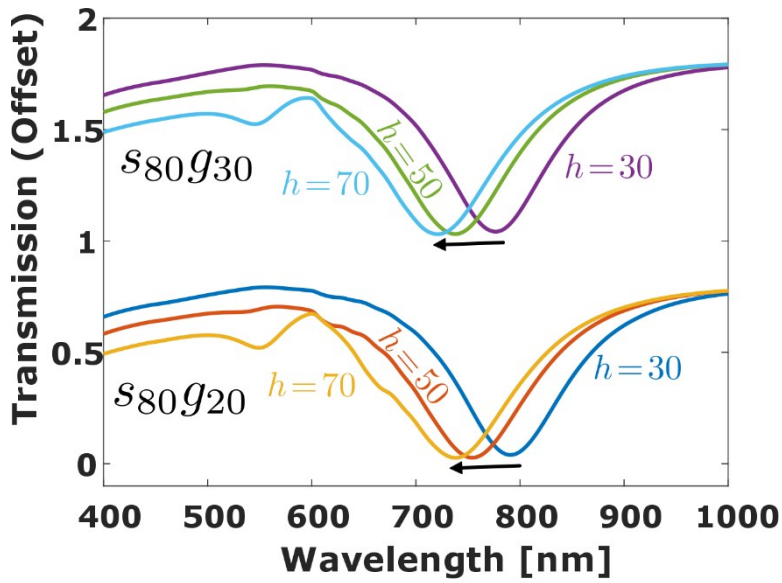


Figure S13. FDTD simulations results showing that the LSP resonance wavelength blueshifts as height increases from *h=30 nm* to *h=70 nm* for both $s_{80}g_{20}$ and $s_{80}g_{30}$ dimer structures.

## Calculation of refractive indexes of AZ5214E

For calculation of the refractive indexes of AZ5214E, we used the Cauchy equation $n(\lambda) = N_1 + N_2\lambda^{-2} + N_3\lambda^{-4}$, with parameters given in the manufacturer's data sheet for unbleached resist: $N_1 =$ 1.6035, $N_2 =$ 0.0055741 μm², and $N_3 =$ 0.00234 μm⁴.